

## How Has The Port City Construction in Colombo, Sri Lanka, Impacted The Spatial and Temporal Dynamics of The Adjacent Coastline?

Geethya Fernando.<sup>1\*</sup>, Ranmalee Bandara.<sup>2</sup>

<sup>1</sup> Department of Remote Sensing and GIS, Faculty of Geomatics, Sabaragamuwa University of Sri Lanka

<sup>2</sup> Department of Surveying and Geodesy, Faculty of Geomatics, Sabaragamuwa University of Sri Lanka

[\\*fernandogeethyathathsarani@gmail.com](mailto:*fernandogeethyathathsarani@gmail.com)

**Abstract:** *In Sri Lanka, due to the Port City construction off the Colombo port, which is a massive anthropogenic intervention and alternation, with large-scale coastal land reclamation, there is concern about the impacts on the adjacent natural coastline dynamics. This research investigated the spatio-temporal coastline variation of the adjacent coastline due to the construction of the Port City in Colombo, Sri Lanka, and identified the relationship between coastline changes from pre-construction to post-construction. Hence, this work developed a method for extracting coastline information using satellite images based on Tasseled Cap Transformation, Otsu image segmentation, and Mathematical morphology, to examine spatial and temporal variation of the coastline from 2007 to 2021. All processing was done using the Google Earth Engine platform and the Geographic Information System software was used to visualize and interpret the results, which were validated with field data. The findings of this study confirmed that anthropogenic activities are a major reason for the adverse impact on the coastline and this method is suitable to detect the coastline changes of large areas within a minimum time period. The results indicate that some specific coastal areas; Mount Lavinia, Dehiwala, and Panadura have accreted coastal region while areas like Galle-face, Wedikanda beach, and Kelani River Estuary have eroded along the coastline after the Port City construction. Further, Negombo beach shows both low erosion and local accretion within the study period. The outcomes of this study are useful for establishing a sustainable coastal management process for effective development in Sri Lanka.*

**Keywords:** *Coastline variation, Colombo Port City construction, Google Earth Engine (GEE), Sri Lanka, Tasseled Cap Transformation (TCT)*

### Introduction

Coastline is the dynamic belt between land and oceans, sensitive to natural and anthropogenic activities (Chen, et al., 2022). Smith and Zartillo, (1990) have defined the instantaneous coastline as the position of the boundary between land and water at instantaneous time. But the definition of the coastline can fluctuate based on factors such as sea level, tides, and currents, and is often described as the point where land and water meet (Toure et al., 2019).

The world economic development associated with coastal areas due to abundant natural marine resources, and various anthropogenic activities interfere with the change of coastline. Specially over-utilization and exploitation of coastal resources might be serious causes like coastal erosion, land area reduction, coastal migration and accumulation so on. These adverse impacts are addressed the coastal areas to become more vulnerable to destruction and escalation of environmental degradation (Yasir et al., 2020).

Port construction and development projects lead to significant alterations in the natural configuration of the coastline (Kudale, 2010). The development of port construction projects consists of constructing coastal infrastructure like breakwaters, jetties, groins, and reclamation bunds and involves dredging and disposal activities (Naik & Kunte, 2016). Tsoukala and Katsardi (2015) have described the reasons for the coastal zone morphology changes due to mega port construction. According to their explanation, any structure or construction in the coastal zone interrupts the longshore current, and those obstructions change the sediment transport patterns. Hence, accretion upstream and erosion downstream can be easily spotted and hard windward surface piercing structures in port constructions might cause diffraction of the waves and alternation of the wave direction. This type of scenario accompanies concentrating wave energy in areas where there was none before the structure was constructed. Installation of heavy equipment, tools, and large-scale machinery in construction sites has a considerable impact on the environment, particularly in the surrounding areas. These industrial activities can alter the topography of coastal land, cause soil erosion, and lead to the depletion of natural resources (Naik & Kunte, 2016).

The Colombo Port City project is Sri Lanka's first large-scale coastal land reclamation initiative, situated near the Colombo port which aims to transform a significant portion of Colombo's coastal area into a new city, complete with modern infrastructure, commercial and residential spaces, and recreational facilities (Gunawansa, 2017). The project's initial plan was drafted in 2011, and in 2013, the Sri Lankan government signed an agreement with a Chinese state-owned construction firm to execute the project. The project involved reclaiming an area of 269 hectares, a total of 65 million cubic meters of marine dredged sand was utilized as the primary material for the land reclamation process (Ranbandara et al, 2021). It involves filling the sea with materials to a depth of 450 meters and creating a landmass that rises 450 meters above ground level. This process also affects the coral reef, which plays a key role in defending the coastline from strong longshore currents. Further, to fill the reclaiming area sand is get from

the offshore sand depositions. Excavating this sand deposition could be a reason to adversely impacted to the sea bed and coastal morphology and extensive mining activities lead to the enlargement of barren sea land (De Silva et al., 2015). Beaven et al. (2018) has highlight that landfills have the potential to cause significant coastal erosion. The establishment and development of an artificial island results in destruction of the natural slope from land to the deep sea and it may aid to deepening the sea and leading break the water waves and it will be redirected to other areas of coastline. Overall, the literature review on the concepts on reclamation and construction of port city project has a major contribution to the coastline variation and this type of scenario accompanies concentrating wave energy in areas where there was none before the structure was constructed.

Even though Port city project is expected to be a significant economic and urban development milestone for Sri Lanka, it couldn't be discarded the potential negative devastating impacts on adjacent coastline area as unimportant or unwanted. Therefore, it should be addressed the impacts on the neighboring coastal areas due to port city construction to ensure the sustainability of the project. Thus, it warrants attention to rapid and replicable identification of the coastline change trends aid in promoting sustainable port management, sand bypassing, dune rehabilitation, and dune vegetation projects. Identifying the coastline dynamic is a vital task in determining the environmental threats and economic vulnerabilities in the western coastal belt due to these kinds of huge anthropogenic activities (De Silva et al., 2015).

This study focuses on detecting the spatial and temporal coastline variation of the adjacent coastlines of the Port City Colombo, from the port city pre construction period to post construction to identify the relationship between coastline variation and anthropogenic activities. The methodological approach for extracting coastline information has developed using remote sensing and GIS technologies as it's encompassed with great potential for detecting and quantifying coastal changes.

## **Literature Review**

### **a. Conventional Methods to Detect Coastline Changes:**

Numerous potential data sources are available for investigate the shoreline, for instance, filed data from beach survey and Geographic Positioning System (GPS), aerial photography, historical photographs, coastal maps, charts, satellite images and variety of digital elevation data obtained from remote sensing platforms (Boak & Turner, 2005). Goldsmith and Oertel (1978), Dolan et al. (1983), Smith and Jackson (1992), Morton (1991), and Overton and Fisher

(1996) have identified challenges of the conventional field surveying, methods, for instance, limited spatial and temporal extent, high expense, labor and time intensive and so on. Byrnes and Anders (1991) have mentioned, aerial photographs are vulnerable to multiple types of distortion, including radial and relief distortion, and variations in scale due to changes in altitude along a flight line that must be adjusted or corrected before use. Manual interpretation for aerial photography and topographic maps is the primary method used for detecting shorelines, whereas it is subjective and relies on the expertise of interpretation and need to have comprehensive knowledge of the particular location, including any influences that could have affected the shoreline's position, such as storms or beach replenishment (Stockdon et al., 2002). Recent field surveying method for mapping the shoreline, employing kinematic differential GPS, installed on a four-wheel-drive vehicle with high level of accuracy (Morton et al., 1993). According to Pajak and Leatherman (2002), this GPS method is more reliable than aerial photography in identifying particular coastline features of significance but expense is still considerable.

#### **b. Remote Sensing and GIS:**

Remote sensing and GIS technologies are increasingly preferred over conventional field surveying methods for continuous monitoring of coastline dynamics due to their ability to overcome the limitations of conventional methods (Zhou et al., 2023). Remote sensing refers to the process of obtaining data or information about a particular object or geographical area without making physical contact, usually by using aircraft or satellites (Chuvieco, 2017). McCarthy et al. (2017) have broadly reviewed the capabilities of remote sensing and Satellite sensors for continuous monitoring and management of shorelines. Multispectral and hyperspectral imagery provide advantages such as covering larger areas and detailed spectral information and limitations of the Remote sensing data source mainly include pixel resolution and its cost. (Boak & Turner, 2005).

#### **c. Automatic Coastline Extraction Methods:**

The advancements in remote sensing and GIS technologies have made automatic coastline extraction more popular (Yasir et al., 2020). Automatic extraction and measuring changes in coastlines involve two stages. As outlined by Ali (2016), the first stage utilizes remote sensing methods to derive coastlines from satellite imagery, and the second stage involves the quantitative evaluation of erosion and accretion rates of the delineated coastlines in both temporal and spatial dimensions which can be performed using Digital Shoreline Analysis

System (DSAS), which was proposed by Thieler and Danforth (1994) and further developed by Thieler et al.(2009). For coastal extraction, remote sensing data is employed with several techniques, such as on-screen digitizing, where one coastline is superimposed on another to visualize temporal variations, being highly subjective and requiring specialized skills (Maiti et al., 2015; Rahman et al., 2011;Ali, 2016). The next method employs unsupervised and supervised classification. In the former, the software automatically groups pixels based on their spectral reflectance properties, while in the latter, the analyst guides the software to categorize land and water cover types (Yu et al., 2011). The third technique is edge detection, which identifies substantial pixel intensity differences between bodies of water and non-water entities. The fourth technique is image segmentation, which separates homogeneous regions as water and non-water and the literature uses various segmentation techniques based on spectral bands and indices such as NDWI and MNDWI for coastal extraction (Yang et al.,2022).

#### **d. Thresholding for Land-Sea Water Segmentation:**

Image segmentation is a process of finding the target region by partitioning pixels into two or more groups based to their characters. Thresholding is a simple and effective method used for segmenting images into different classes by utilizing a histogram to mine spectral information (Goh et al.,2002). Toure et al.(2019) described methods of image segmentation for shoreline extraction using band thresholding either manual input or a locally adaptive approach to select a threshold value that aims to segregate the image into land and water elements. Jishuang and Chao (2002), Aedla et al. (2015) have proposed different approaches such as multi threshold based morphological and adaptive thresholding for shoreline detection. Otsu's method, proposed by Otsu (1979), widely uses the image histogram to generate a binary image by identifying the threshold value that maximizes the between-class variance of the target and background and, is effective in achieving uniformity and shape measures from the images (Mutanga & Kumar, 2019). However, thresholding methods may not be sufficient for multispectral and hyperspectral images due to the intricacy of the information. When it comes to multispectral and hyperspectral images, thresholding methods may be inadequate due to the intricate nature of the information (Toure et al., 2019). The threshold value determination directly affects the accuracy, and it is necessary to select an appropriate threshold value through accurate measurements from the experimental results (Tang et al., 2022).

**e. Tasseled Cap Transformation:**

Kauth and Thomas (1976) introduce a concept called the "Tasseled Cap Transformation" which can simplify and summarize the data from the satellite imagery, making it easier to analyze and interpret. The Tasseled Cap Transformation (TCT) involves a mathematical formula that reduces the data to six values or "coefficients," which represent different aspects of the spectral-temporal. Later research, reveal that the TCT is widely used for analyzing and interpreting multispectral remote sensing data, and it is based on the three main components of brightness, greenness, and wetness. Baig et al.(2014) derives a new TCT for Landsat 8 based on the at-satellite reflectance data, which can be directly used for image analysis without the need for atmospheric correction.

Chen et al.(2019) introduced a new method for extracting coastline information from Landsat-8 OLI satellite imagery. The authors use the TCT and mathematical formula that simplifies and summarizes satellite data, to identify the coastline in the images. The authors demonstrate the effectiveness of this method by analyzing Landsat-8 OLI images of the coastline in the Fujian Province of China. They compared the results of their method with other methods, including a manual interpretation by experts, and find that their method produces accurate and reliable results. Further Chen et al.(2022) developed the method of extracting water body information from remote sensing imagery using the newly derived TCT for Landsat 8 based on satellite reflectance data. The authors applied the concepts of "greenness" and "wetness" into the TCT to enhance the accuracy of water body extraction by analyzing Landsat-8 OLI images of two different regions in China and comparing the results with other remote sensing methods. The literature concluded that the TCT is a useful tool for extracting coastline information from satellite imagery, as it simplifies the data and provides a clear visualization of the coastline.

**f. Edge Detection:**

Edges in an image refer to significant local changes in intensity, found at the boundary between two different regions. The identification of edges is an essential step in shoreline detection. Many edge detection techniques have been developed for coastline detection, including the Canny edge detector. The challenge is an adjustment of the associated parameters, which is a complex task that significantly impacts the results (Gupta,2016).

The Canny edge detector algorithm is commonly employed for extracting water features, along with the Otsu algorithm to calculate the threshold value (Canny, 1986), Zhang et al. (2012) and

Kuleli et al. (2011) utilized the Otsu algorithm within the Canny edge detection model to detect the shoreline, respectively. Zhang et al. (2012) implemented this approach to identify the coastlines along the Qinhuangdao coastline in China, while Kuleli et al. (2011) applied the same method to detect shorelines in the Ramsar wetlands of Turkey.

**g. Mathematical Morphology:**

Mathematical morphology (MM) is a branch of image processing, deals with the analysis and manipulation of geometric structures, such as edges, boundaries, and shapes (Serra & Soille, 2012). MM techniques are particularly useful for coastline extraction because they can preserve the edges and shapes of water bodies while removing noise and other unwanted features. MM operations, such as erosion and dilation, remove small objects and fill gaps in water bodies, resulting in a more accurate coastline extraction and it allows analysis of water bodies based on their size and shape, which can be useful for characterizing the temporal and spatial evolution of coastlines. By applying MM techniques to remotely sensed images, coastline information can be extracted automatically and accurately, allowing for the efficient monitoring of coastal areas (Chen et al., 2022). Rishikeshan and Ramesh (2018) presents an automated algorithm for extracting water bodies from remotely sensed images using MM with several processing steps including noise removal, image enhancement, image segmentation, and post-processing. Bagli & Soille, (2003) drove an approach to the coastline extraction using Landsat 7 satellite images using MM strategies for the entire European Continent

**h. Google Earth Engine and LANDSAT Data:**

The Google Earth Engine (GEE) is a web-based online cloud computing platform that offers access to a vast collection of satellite imagery, raster data, and vector data covering various locations worldwide for open source use (Gorelick et al., 2017). The cloud-based computing services, enabling users to process large amounts of geospatial data and access to software and algorithms. The data repository contains a comprehensive collection of satellite data from various sources over 40 years and covering the entire globe at different temporal resolutions (Mutanga & Kumar, 2019).

Landsat is one of the major Earth observing satellite mission continuously available data since 1972 (Williams et al., 2006). Most studies have engaged with Landsat data for time series detection purposes due long term availability, publicly accessible and free of charge data (Wulder et al., 2019). Chen et al. (2019) have used Landsat 8 data to extract coastline in Yangtze River Estuary in China while Colak et al. (2019) have used Landsat 8 data for extract coastline



of Bodrum Peninsula in Turkey. Further, Gonçalves et al.(2015) extracted the coastline from Landsat 8 images considering high and low tide 75km of sandy beach in Portuguese. The use of high-resolution satellite data is less common in published research, likely due to the notable high cost accompanied with acquiring such data.

## Methodology

### a. Study Area:

This study significantly targeted the vicinity of the Colombo Port city, Sri Lanka, the largest and most prominent coastal engineering construction area, off to Colombo port. The Study Area is extended from the estuary of Maha oya ( $7^{\circ}16'14.87''\text{N}$ ,  $79^{\circ}50'30.43''\text{E}$ ) to the estuary of Kalu ganga ( $6^{\circ}35'17.23''\text{N}$ ,  $79^{\circ}57'18.31''\text{E}$ ) along the western coastline belt. This coastline is contiguous with the three most urbanized districts in Sri Lanka which are Colombo, Kalutara and Gampaha. The study region has a tropical maritime climate with an average temperature of  $27^{\circ}\text{C}$  on the western coasts. Rainfall exhibits a seasonal pattern, influenced by the monsoon system. The variations in weather conditions are predominantly caused by the south-western monsoon, which occurs from May to September (Abeykoon et al., 2021).

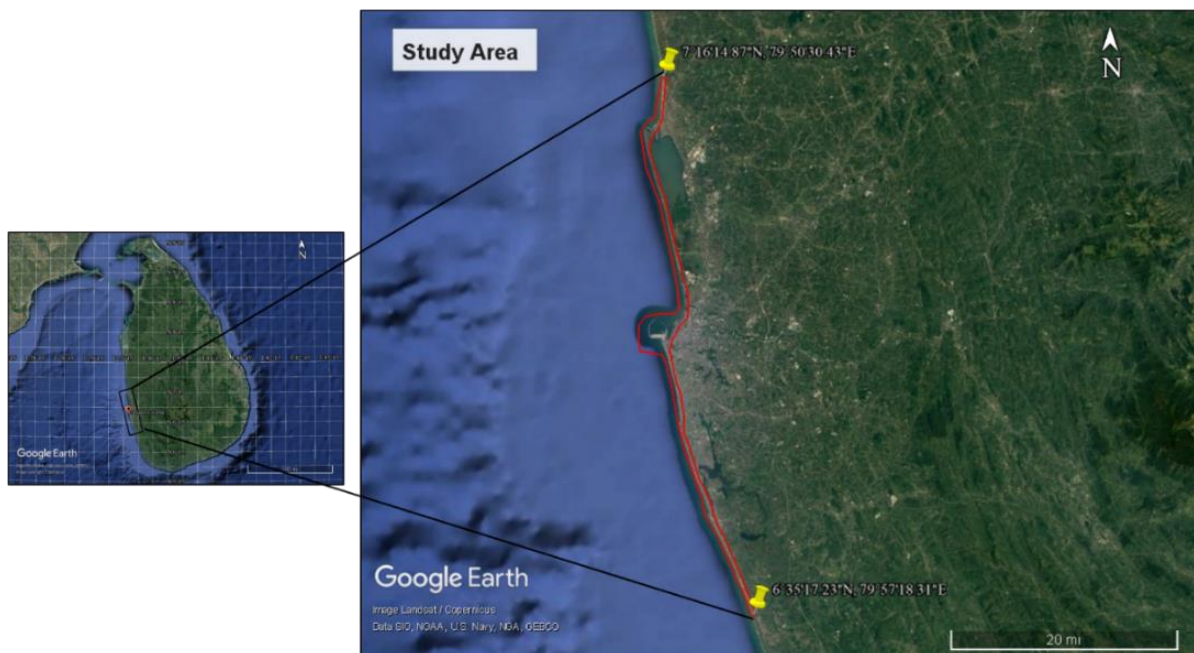


Figure 1: The study area along the western coastal belt, Sri Lanka

### b. Data Pre-Processing:

The initial pre-processing stage involves the satellite image orthorectification, and coregistration, namely atmospheric correction, Radiometric calibration and conversion to top-



of-atmosphere (TOA) reflectance. These steps are essential to ensure that the data acquired on multiple dates overlap. GEE platform performs these steps internally and seamlessly during data ingestion from the USGS (United States Geological Survey) repository.

Orthorectification step involves removing geometric distortion arising from factors such as the Earth's surface curvature, terrain relief, and the satellite sensor orientation. Image registration involves aligning the different Landsat 8 images taken at different times to a common reference frame. This is necessary for accurate comparison of the images and detection of changes over time (Gao et al., 2023). Atmospheric correction is necessary to remove the effects of atmospheric conditions on the satellite images and it can improve the accuracy of spectral analysis and change detection. Radiometric calibration step involves converting the raw digital number (DN) values of the Landsat 8 images to TOA reflectance values. This process allows for better comparison of different images taken at different times, as TOA reflectance values are less influenced by differences in atmospheric conditions (Chen et al., 2022).

The relevant tiles covering the study area were identified by filtering the data collection using the Worldwide Reference System (WRS) based on path 141 and row 55. The Landsat 8 OLI (Operational Land Imager) and Landsat 5 TM (Thematic Mapper) images from the GEE data catalog were filtered for the selected time period, January to February in each year during the study period. This strategy was used to reduce the impact of seasonal variations and other short-term changes in the data. It obtains the long-term trends and patterns of the data using time-series analysis with minimal errors. It ensures consistency in the data and makes comparing different time periods easier. The study area was defined using Google Earth Pro software and the shapefile was imported to the GEE asset to extract the data for the desired area. The filtered data list for each year was visually inspected to obtain the cloud-free images within the study area which may not hinder the identification of coastline changes.

### **c. Data Processing:**

TCT coefficient, corresponding to the satellite sensor was applied to each preprocessed remote sensing image. This transformation compressed the Satellite remote sensing imagery, which produces a set of components corresponding to a weighted index, allowing each pixel to be reflected in the original multispectral image. This transformation can be represented by an equation in the form of  $y = cx + a$ , where  $y$  represents the component in multispectral space after the transformation,  $x$  is the original multispectral bands,  $c$  is the transformation coefficient that is dependent on the onboard sensor, and  $a$  is a constant that is used to prevent negative

values. After implement the TCT coefficient for each satellite image, it produces the new spectral space where the first three components are significant. These components are brightness, greenness and wetness. The brightness component represents the bare soil, while the greenness component is associated with vegetation cover, biomass, and leaf base cover index. The wetness component shows the moisture status of ground objects. Wetness coefficient derived from Tasselled Cap analysis was employed to identify and detect open water surfaces for this study (Chen et al., 2022).

The wetness band was subjected to automatic image thresholding using the Otsu method. To achieve this, a single-band image was generated by choosing the wetness coefficient band, which was used to determine the threshold value for distinguishing water from land. The threshold value for separating water from land was determined automatically by iteratively applying the Otsu method on the histogram of the wetness band. The resulting threshold value was used to create the binary image of the wetness band. In this binary image, one class contains pixels with wetness values below the threshold while the other class contains pixels with higher wetness values. The resulting binary image is then added to the map as a layer and mathematical morphology opening and closing operations were used to fill small holes, remove small objects, and smooth the edges. All output data were exported with WGS 84 / UTM zone 44N projected coordinate system (EPSG:32644) and exported results from the GEE were opened in a GIS software, for further analysis and visualization.

#### **d. Data Visualization and Interpretation:**

In the visualization stage, processed satellite data from GEE in raster file format were imported into the GIS software. In order to perform spatial analysis, raster data were then converted to vector format using the Polygonize tool. The next step involved using the Polygon to Lines tool to convert the polygon features into polyline features and the coastline was selected and exported as a line feature. Finally, the exported line features were used to design map layouts are grid index maps to the interpret the obtained results.

#### **e. Validation:**

The validation was carried out by using field data, received as beach profiles from National Aquatic Resources Research and Development Agency, Sri Lanka. Firstly, the High-Water Level (HLW) point coordinates have been identified using the beach profile. Identified coordinates were listed in csv file format and imported into GIS platform to plot the points.

Then the comparison was made between coastline extracted from the automated methodology with the data points obtained from the field.

### Results and Discussion

To achieve the ultimate goal of the study, to examine the potential effects due to mega coastal development on the adjacent coastline from pre-construction to post-construction, the methodology was implemented for the study period of 2007 to 2021. **Figure 2** Shows the outputs from the key methodological steps in GEE.

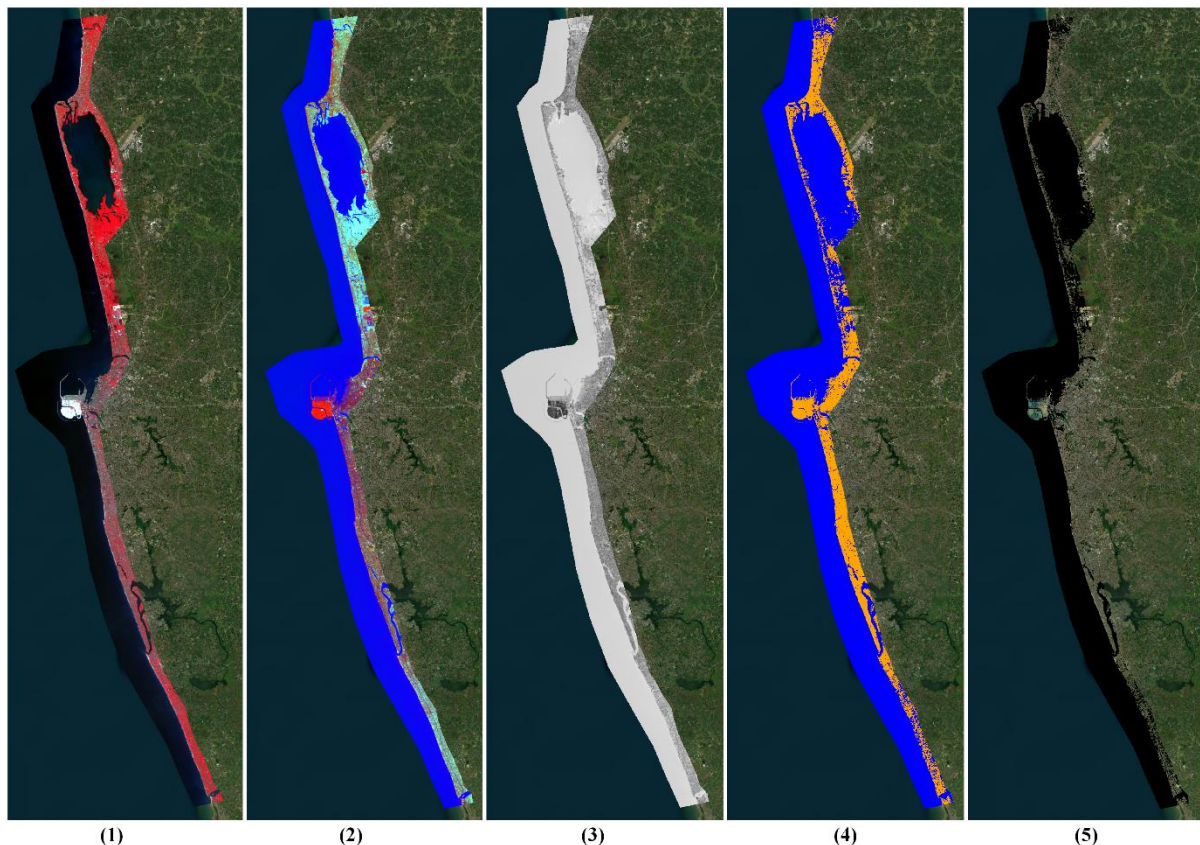


*Figure 2: The Outputs from the Key Methodological Steps in GEE*

In Figure 2 (1) displays the preprocessed satellite image using false color composite using near infrared, red, and green bands for year 2021, clipped to the study area. Red color represents vegetation, cyan blue represents urban areas, and black represents water bodies. False color composite of the Landsat 5 combination with Band4, Band3 and Band2 while Landsat 8 composite with Band5, Band4, Band3. Figure 2 (2) step Showcases the resulting images after implementing TCT analysis, which reduces multispectral data from satellite images to a set of three uncorrelated components: brightness, greenness, and wetness The red color indicates the brightness band, which can identify bare soil and urban areas while greenness band can be used

to identify vegetation, and wetness band with blue color is used to separate water features analyzing the moisture content of the image in order to distinguish between wet and dry land. The step (3) of Figure 2 represents wetness band selected from the TCT Image which separate the study area into wet and dry land. According to the statistical histogram of the wetness band for the year 2021, the most frequent wetness data is notable within the approximate range of 0.039 to 0.059 while highest frequency value in the band is 0.043. Analysing the histogram of the Wetness band is important to calculate the threshold value. In Figure 2 (4) step, implemented Otsu image segmentation to determine optimal threshold value by analyzing the histogram of the wetness band and resulting image provide a binary image, separate the study area into two segments; wet land and dry land. blue color indicates the presence of wet land with water features, while the orange color is assigned to the dry area. When comparing step (4) with (3) and (2), it becomes clear to distinguish between the water and non-water areas.

The binary image resulting from step Figure 2 (4) subjected to the post-processing step with implementing mathematical opening and closing operations The resulting image Figure 2 (5) represents the binary image where the foreground and background values indicating 1 and 0 respectively. The morphological operations were used to get the fine coastline while removing the noise formed by lakes, rivers, reservoirs, and fill holes caused by ships. This same procedure was done for other years also;2007,2010,2014,2016 and 2018 in GEE platform and visual interpretation and outcomes were performed in GIS platforms.

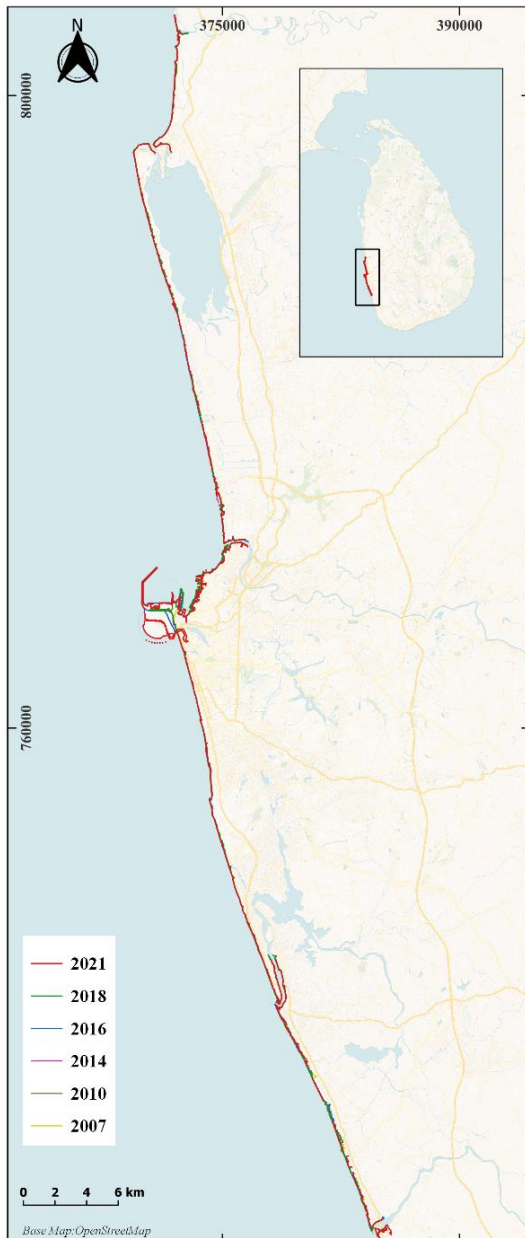


*Figure 3: Time series of extracted coastlines in the study area.*

**Figure 3** has layout the extracted coastline for year 2007, 2010, 2014, 2016, 2018 and 2021 by georeferencing the coordinate, which can be used to visually identified there are some variations had occurred between each coastline. However, it can be inferred that the coastlines do not firmly overlap, indicating the presence of some variations. Further, it can be noticed that there are some discontinuities in the coastline holdings with missing data. The missing data could be associated with various factors such as cloud cover or mist during the image capture by the satellite.

The **Figure 4** present several significant areas which are considered in this study to examine the coastal evaluation from 2007 to 2021. It can be observed that there is a disparity between the actual shape of the base map features and the generated coastline. This disparity is possible because the wetness band calculates the moisture content at the time the image is taken, and it is possible that the area might experience subsidence from the sea current or the water may extend beyond the actual edge of the area, or edges may be saturated with water and the basemap is related to the year 2023, since the extracted coastlines are from the years 2007 and 2021.

The coastal areas of Negombo in the Gampaha district experience both minimum erosion and accretion as shown in **Figure 4** (a). Based on existing literature, the reason for these minimal changes could be due to implementation of coastal protection techniques in the Negombo coastal area (Abeykoon et al., 2021).



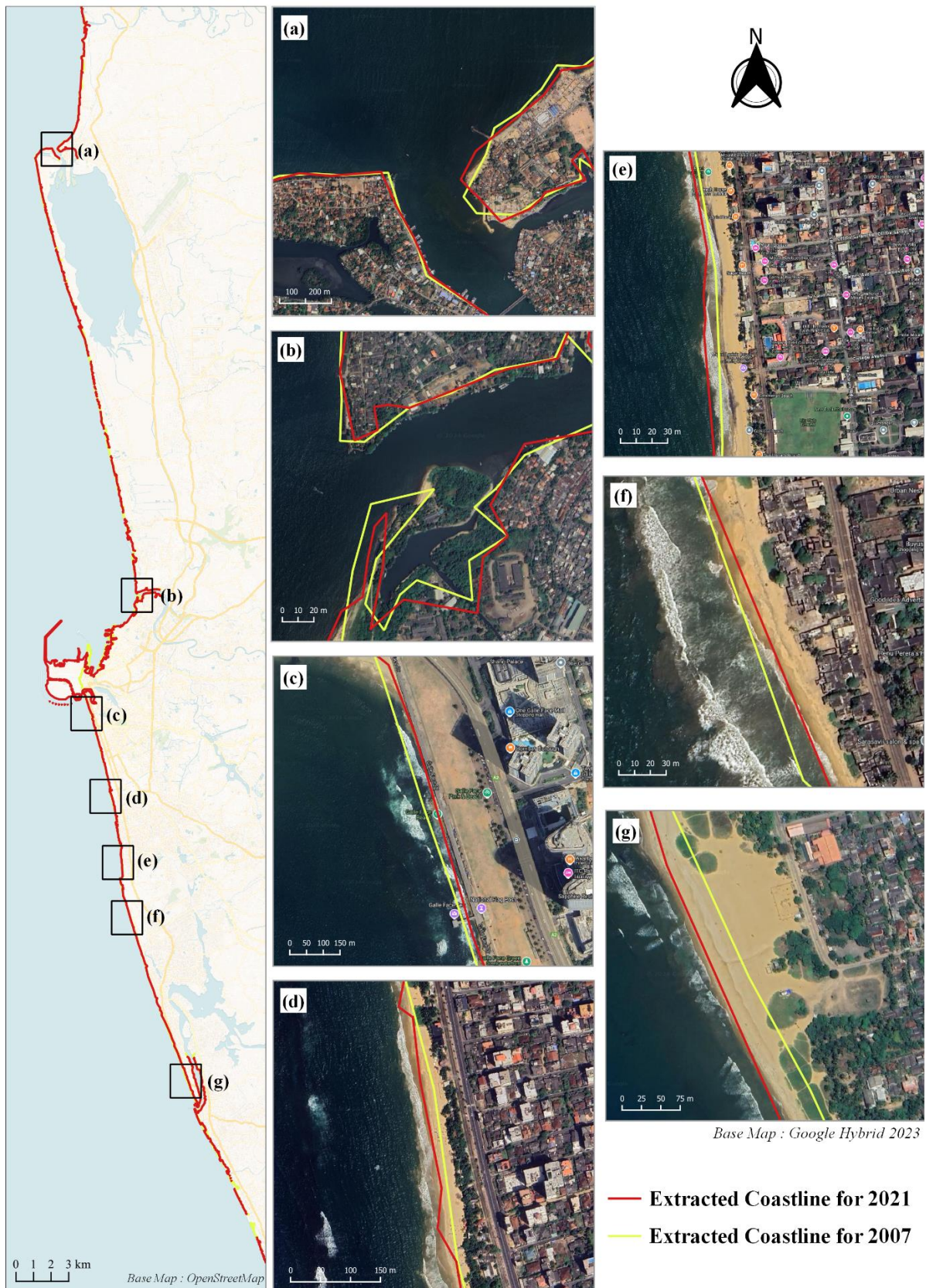


Figure 4: Coastline Changes from 2007 to 2021. (a) Coastal area of Negombo, (b) Coastal area of Estuary of Kelani River, (c) Coastal area of Galle Face, (d) Coastal area of Dehiwala, (e) Coastal area of Mount Lavinia, (f) Coastal area of Wedikanda, (g) Coastal area of Panadura.



The study area includes several estuaries including Kalani river estuary, Kalu ganga estuaries and Maha oya estuary which are major contributor to balancing the sediment levels. Despite the fact that river estuaries can contribute to maintaining a balance in the sediment budget, a reduction in the coastline has been observed in the vicinity of the Kelani River estuary from this study (**Figure 4 (b)**). However, various studies such as Dissanayake and Rupasinghe (1996), Piyadasa (2011) and Dayananda (1992) have shown that sand mining including Kalani river, Kalu ganga, Maha oya and other major rivers have led to reduced sediment transportation, disturbing the natural balance and resulting in coastline erosion.

In **Figure 4 (c)** image shows the area of Galle Face that is close proximity to Colombo port city. Moderate erosion can be observed when comparing the coastline of 2007 with the coastline of 2021. Although the changes may be moderate, they should be taken into account due to the significance of this area as one of the most important beaches in Sri Lanka. Affiliated with the port city construction, a breakwater has also been designed to hinder the waves that strike the coast from reaching the Port City site. In addition to that, besides the construction of the port city, the development of the Colombo South Port construction with its particular breakwater has also taken place. This kind of large breakwater can contribute to the erosion of the coastline adjacent to it. While substantial evidence has been provided by (Abeykoon et al., 2021), that the utilization of hard structures has adverse impacts on the coastal scenery, it can be concluded that coastal erosion occurred between 2007 and 2021 in Galle Face Beach due to the construction of revetments and huge breakwaters as the part of Port City project and Colombo's commercial harbor. These structures potentially disrupt the transport of sediment along the shoreline and are susceptible to the influence of seasonal winds (Tsoukala & Katsardi, 2015).

It is observable possible erosion are happened in the Wedikanda Beach in **Figure 4 (f)**. According to the study of Abeykoon et al. (2021) the highest EPR value in the Colombo district was recorded in the Wedikanda-North region with a value of 4.29 m yr<sup>-1</sup>, making it more susceptible to erosion.

The comparison of the two coastlines (2007 and 2021) reveals that variations are happen accreting the coastline in the area of Dehiwala (**Figure 4(d)**), Mount Lavinia (**Figure 4(e)**) and Panadura area (**Figure 4(g)**) with the time scale. According to the study results of Lakmali et al. (2017), several locations were covered namely Dehiwala, Mount Lavinia, Wellawatta, Wadduwa, Rathmalana, and Hikkaduwa can see huge seasonal erosion, but according to the

author's perspective it has identified that they are only seasonal changes and it gets recovered and accreted after the season. However, the results present significant coastline accretion with time factor. Whether it is not a desired result, the possibility of that accretion can be proved by the study of Lakmali et al. (2017). They have highlighted that the Dehiwala, Mount Lavinia, and Panadura beaches are not a constant occurrence or permanent phenomenon and their effect varies depending on the season. The accretion of these beaches is observed during the initiation of the fair-weather north-eastern monsoon.

### **Conclusion and Recommendation**

The study has identified the accreted and eroded from pre-construction to the post-construction of the port city Colombo, Sri Lanka. The findings of this study highlight that the changes in the coastline area of Galle face have moderate erosion while the Estuary of Kelani River has low erosion. Wedikanda beach also shows possible erosion through this outcome. The area of Mount Lavinia and Dehiwala has Moderate accretion while Panadura gains more accretions of the coastline. Further, Negombo beach area shows both low erosion and accretions regionally. By addressing these results, it could be concluded that studied area have been caused by human activities or interventions, specifically port city construction either directly or indirectly. Additionally, natural factors such as natural barriers, coral reefs, tidal fluctuations, longshore currents, rising sea levels, climate change, and other similar events also have contributed for these results. It is crucial to verify the changes are only affected due to anthropogenic activities, caused by anthropogenic interventions and natural phenomena that are interconnected. But scientifically, it can be concluded that anthropogenic activities are more prominent factor for the cause of coastal variation, rather than natural events of the studied region. However, currently there is no definitive scientific proof regarding the impact of the Port City on coastal erosion on the western coastline. Only theoretical assumptions can be made based on analyzing potential technical arguments.

Based on the Outcomes of this study, it's suggested to implement coastal conservation technologies for these eroded areas in the western coastal belt, to prevent drastic damages in the future. It is recommended to apply the methodological approach used in this study to automate the long-term time series analysis for the large coastal area. However, there are some limitations of this study due to the spatial and temporal gaps of the Landsat Satellite data and cloud cover. Therefore, it's suggested to use high resolution satellite imagery instead of 30m resolution images with the same satellite sensor throughout the study period with minimum

cloud cover or apply possible cloud removing methods. With high-resolution imageries tidal effecting could be a prominent factor to affect the accuracy of the coastline extraction. So, it is recommended to taking into account tidal correction when following this method. As a future direction, it is proposed to further develop this methodology, considering current patterns, sea level rise, climate changes and quantify coastal change tendency.

## References

1. Abeykoon, L. C. K., Thilakarathne, E. P. D. N., Abeygunawardana, A. P., Warnasuriya, T. W. S., & Egodaunya, K. P. U. T. (2021). *ARE COASTAL PROTECTIVE HARD STRUCTURES STILL APPLICABLE WITH Asian Development Bank Institute* (Issue April).
2. Aedla, R., Dwarakish, G. S., & Reddy, D. V. (2015). Automatic Shoreline Detection and Change Detection Analysis of Netravati-GurpurRivermouth Using Histogram Equalization and Adaptive Thresholding Techniques. *Aquatic Procedia*, 4(Icwrcoe), 563–570. <https://doi.org/10.1016/j.aqpro.2015.02.073>
3. Ali, A. R. (2016). *Assessing Change and Vulnerability of the Guyana Coastline with Multi-Temporal Landsat Imagery and Survey Data* (Master's thesis, University of Windsor (Canada)).
4. Anders, F. J., & Byrnes, M. R. (1991). Accuracy of shoreline change rates as determined from maps and aerial photographs. *Shore and Beach*, 59(1), 17-26.
5. Bagli, S., & Soille, P. (2003). Morphological automatic extraction of coastline from pan-European Landsat TM images. *Proceedings of the Fifth International Symposium on GIS and Computer Cartography for Coastal Zone Management* (<http://Www.Gisig.It/Coastgis/>), 1998, 58–59.
6. Baig, M. H. A., Zhang, L., Shuai, T., & Tong, Q. (2014). Derivation of a tasseled cap transformation based on Landsat 8 at-satellite reflectance. *Remote Sensing Letters*, 5(5), 423–431. <https://doi.org/10.1080/2150704X.2014.915434>
7. Beaven, R. P., Kebede, A. S., Nicholls, R. J., Haigh, I. D., Watts, J., & Stringfellow, A. (2018). *Coastal Landfill and Shoreline Management: Implications for Coastal Adaptation Infrastructure Case Study: Pennington*. 37.
8. Boak, E. H., & Turner, I. L. (2005). Shoreline definition and detection: A review. *Journal of Coastal Research*, 21(4), 688–703. <https://doi.org/10.2112/03-0071.1>
9. Byrnes, M. R., & Anders, F. J. (1991). Accuracy of Shoreline Change Rates as Determined from Maps and Aerial Photographs. *Shore and Beach, January 1991*, 17–26. <https://www.researchgate.net/publication/284041608>
10. Canny, J. (1986). A computational approach to edge detection. *IEEE Transactions on pattern analysis and machine intelligence*, (6), 679-698.
11. Chen, C., Chen, H., Liang, J., Huang, W., Xu, W., Li, B., & Wang, J. (2022). Extraction of Water Body Information from Remote Sensing Imagery While Considering Greenness and Wetness Based on Tasseled Cap Transformation. *Remote Sensing*, 14(13), 3001. <https://doi.org/10.3390/rs14133001>
12. Chen, C., Fu, J., Zhang, S., & Zhao, X. (2019). Coastline information extraction based on the tasseled cap transformation of Landsat-8 OLI images. *Estuarine, Coastal and Shelf Science*, 217, 281–291. <https://doi.org/10.1016/j.ecss.2018.10.021>

13. Chen, C., Liang, J., Xie, F., Hu, Z., Sun, W., Yang, G., ... & Zhang, Z. (2022). Temporal and spatial variation of coastline using remote sensing images for Zhoushan archipelago, China. *International Journal of Applied Earth Observation and Geoinformation*, 107, 102711.
14. Chuvieco, E. (2017). *FUNDAMENTALS OF SATELLITE REMOTE SENSING With the collaboration of. March.*
15. Colak, T. I., Senel, G., & Goksel, C. (2019). Coastline zone extraction using Landsat-8 OLI imagery, case study: Bodrum Peninsula, Turkey. *International Archives of the Photogrammetry, Remote Sensing and Spatial Information Sciences - ISPRS Archives*, 42(4/W12), 101–104. <https://doi.org/10.5194/isprs-archives-XLII-4-W12-101-2019>
16. Dayananda, H. V. (1992). *Shoreline Erosion in Sri Lankas's Coastal Areas*. 72. [https://pdf.usaid.gov/pdf\\_docs/pnabs575.pdf](https://pdf.usaid.gov/pdf_docs/pnabs575.pdf)
17. De Silva, S. U., Sachindrani, D., Hatharasinghe, H., & Bogahawatte, I. (2015). *The Contradiction between Sustainable Development and Economic Development: Special Reference to the Colombo Port City Project of Sri Lanka*. November, 196–201.
18. Deepa, N., & Kunte, P. D. (2016). Impact of port structures on the shoreline of Karnataka, west coast, India.
19. Dissanayake, C. B., & Rupasinghe, M. S. (1996). Environmental impact of mining, erosion and sedimentation in Sri Lanka. *International Journal of Environmental Studies*, 51(1), 35–50. <https://doi.org/10.1080/00207239608711069>
20. Dolan, R., Hayden, B., & May, S. (2018). Erosion of the US shorelines. In *Handbook of Coastal Processes and Erosion* (pp. 285-300). CRC Press.
21. Gao, F., Masek, J. G., & Wolfe, R. E. (2009). Automated registration and orthorectification package for Landsat and Landsat-like data processing. *Journal of Applied Remote Sensing*, 3(1), 033515.
22. Goh, T. Y., Basah, S. N., Yazid, H., Safar, M. J. A., & Saad, F. S. A. (2018). Performance analysis of image thresholding: Otsu technique. *Measurement*, 114, 298-307.
23. Goldsmith, V., & Oertel, G. (1978). Beach profiling. In *Standards for Measuring Shoreline Changes: Proceedings of a Workshop*. Tallahassee, Florida: Geology Department, Florida State University (pp. 37-41).
24. Gonçalves, G., Duro, N., Sousa, E., & Figueiredo, I. (2015). Automatic extraction of tide-coordinated shoreline using open source software and Landsat imagery. *International Archives of the Photogrammetry, Remote Sensing and Spatial Information Sciences - ISPRS Archives*, 40(7W3), 953–957. <https://doi.org/10.5194/isprsarchives-XL-7-W3-953-2015>
25. Gorelick, N., Hancher, M., Dixon, M., Ilyushchenko, S., Thau, D., & Moore, R. (2017). Remote Sensing of Environment Google Earth Engine : Planetary-scale geospatial analysis for everyone. *Remote Sensing of Environment*, 2016. <https://doi.org/10.1016/j.rse.2017.06.031>
26. Gunawansa, A. (2017). *Creation of New Urban Land by Reclaiming the Sea in Colombo Port City, Sri Lanka*. 98–119. [https://unhabitat.org/sites/default/files/download-manager-files/1544097120wpdm\\_Colombo Case Study.pdf](https://unhabitat.org/sites/default/files/download-manager-files/1544097120wpdm_Colombo Case Study.pdf)
27. Gupta, R. (2016). Enhanced edge detection technique for satellite images. In *Cloud Computing and Security: Second International Conference, ICCCS 2016, Nanjing, China, July 29-31, 2016, Revised Selected Papers, Part I 2* (pp. 273-283). Springer International Publishing.
28. Jishuang, Q., & Chao, W. (2002). a Multi-Threshold Based Morphological Approach for Extracting Coastal Line Feature in Remote Sensed Images. *FIEOS 2002 Conference Proceedings, I*. <http://www.wins.uva.nl/research/isis>

29. Kauth, R. J. (1976). *Tasselled Cap - a Graphic Description of the Spectral-Temporal Development of Agricultural Crops As Seen By Landsat*. 41–51.
30. Kudale, M. D. (2010). Impact of port development on the coastline and the need for protection. *Indian Journal of Marine Sciences*, 39(4), 597–604.
31. Kuleli, T., Guneroglu, A., Karsli, F., & Dihkan, M. (2011). Automatic detection of shoreline change on coastal Ramsar wetlands of Turkey. *Ocean Engineering*, 38(10), 1141–1149. <https://doi.org/10.1016/j.oceaneng.2011.05.006>
32. Lakmali, E. ., Deshapriya, W. G. ., Ishara Jayawardene, K. G. A., Raviranga, R. M. ., Ratnayake, N. ., Premasiri, H. M. ., & Senanayake, I. . (2017). Long term coastal erosion and shoreline positions of Sri Lanka. *Journal of Survey in Fisheries Sciences*, 3(2). <https://doi.org/10.18331/sfs2017.3.2.1>
33. Williams, D. L., Goward, S., & Arvidson, T. (2006). Landsat. *Photogrammetric Engineering & Remote Sensing*, 72(10), 1171-1178.
34. Maiti, S., Jha, S. K., Garai, S., Nag, A., Chakravarty, R., Kadian, K. S., Chandel, B. S., Datta, K. K., & Upadhyay, R. C. (2015). Assessment of social vulnerability to climate change in the eastern coast of India. *Climatic Change*, 131(2), 287–306. <https://doi.org/10.1007/s10584-015-1379-1>
35. McCarthy, M. J., Colna, K. E., El-Mezayen, M. M., Laureano-Rosario, A. E., Méndez-Lázaro, P., Otis, D. B., Toro-Farmer, G., Vega-Rodriguez, M., & Muller-Karger, F. E. (2017). Satellite Remote Sensing for Coastal Management: A Review of Successful Applications. *Environmental Management*, 60(2), 323–339. <https://doi.org/10.1007/s00267-017-0880-x>
36. Meng, F., & Li, A. (2018). Pavement Crack Detection Using Sketch Token. *Procedia Computer Science*, 139, 151–157. <https://doi.org/10.1016/j.procs.2018.10.231>
37. Morton, R. A., Leach, M. P., Paine, J. G., & Cardoza, M. A. (1993). Monitoring beach changes using GPS surveying techniques. *Journal of Coastal Research*, 9(3), 702–720.
38. Morton, R.A., 1991, June. Accurate shoreline mapping: past, present, and future. In *Coastal sediments* (pp. 997-1010). ASCE.
39. Mutanga, O., & Kumar, L. (2019). Google earth engine applications. In *Remote Sensing* (Vol. 11, Issue 5). <https://doi.org/10.3390/rs11050591>
40. Naik, D., & Kunte, P. D. (2016). Impact of Port Structures on the Shoreline of Karnataka, West Coast, India. *International Journal of Advanced Remote Sensing and GIS*, 5(1), 1726–1746. <https://doi.org/10.23953/cloud.ijarsg.56>
41. Ostu, N. (1979). A threshold selection method from gray-level histograms. *IEEE Trans SMC*, 9, 62.
42. Overton, M. F., & Fisher, J. S. (1996). Shoreline analysis using digital photogrammetry. In *Coastal Engineering 1996* (pp. 3750-3761).
43. Pajak, M. J., & Leatherman, S. (2002). The high water line as shoreline indicator. *Journal of Coastal Research*, 18(2), 329–337.
44. Piyadasa, R. U. K. (2011). River sand mining and associated environmental problems in Sri Lanka. *IAHS-AISH Publication*, 349, 148–153.
45. Rahman, A. F., Dragoni, D., & El-Masri, B. (2011). Response of the Sundarbans coastline to sea level rise and decreased sediment flow: A remote sensing assessment. *Remote Sensing of Environment*, 115(12), 3121–3128. <https://doi.org/10.1016/j.rse.2011.06.019>
46. Ranbandara, P. G. G. M., Thilakarathne, R. U., Athapaththu, A. M. R. G., Kurukulasooriya, L. C., & Gonaduwege, B. P. Examination on Geotechnical Properties of Marine Dredge Sand of Colombo Port City.
47. Rishikeshan, C. A., & Ramesh, H. (2018). An automated mathematical morphology driven algorithm for water body extraction from remotely sensed images. *ISPRS Journal of*



- Photogrammetry and Remote Sensing*, 146(August 2017), 11–21. <https://doi.org/10.1016/j.isprsjprs.2018.08.014>
48. Serra, J., & Soille, P. (Eds.). (2012). *Mathematical morphology and its applications to image processing* (Vol. 2). Springer Science & Business Media.
  49. Smith, A. W. S., & Jackson, L. A. (1992). The variability in width of the visible beach. *Shore and Beach*, 60(2), 7-14.
  50. Smith, G. L., & Zarillo, G. A. (1990). Calculating long-term shoreline recession rates using aerial photographic and beach profiling techniques. *Journal of coastal research*, 111-120
  51. Stockdonf, H. F., Sallenger Jr, A. H., List, J. H., & Holman, R. A. (2002). Estimation of shoreline position and change using airborne topographic lidar data. *Journal of Coastal Research*, 502-513.
  52. Tang, W., Zhao, C., Lin, J., Jiao, C., Zheng, G., Zhu, J., Pan, X., & Han, X. (2022). Improved Spectral Water Index Combined with Otsu Algorithm to Extract Muddy Coastline Data. *Water (Switzerland)*, 14(6), 1–15. <https://doi.org/10.3390/w14060855>
  53. Thieler, E. R., & Danforth, W. W. (1994). Historical shoreline mapping (I): improving techniques and reducing positioning errors. *Journal of Coastal Research*, 549-563.
  54. Thieler, E. R., Himmelstoss, E. A., Zichichi, J. L., & Ergul, A. (2009). *The Digital Shoreline Analysis System (DSAS) version 4.0-an ArcGIS extension for calculating shoreline change* (No. 2008-1278). US Geological Survey.
  55. Toure, S., Diop, O., Kpalma, K., & Maiga, A. S. (2019). Shoreline detection using optical remote sensing: A review. *ISPRS International Journal of Geo-Information*, 8(2), 75.
  56. Tsoukala, V. K., & Katsardi, V. (2015). *Beach Erosion and Consequential Impacts Due to the Presence of Harbours in Sandy Beaches in Greece and Cyprus*. 2, 55–71. <https://doi.org/10.1007/s40710-015-0096-0>
  57. Wulder, M. A., Loveland, T. R., Roy, D. P., Crawford, C. J., Masek, G., Woodcock, C. E., Allen, R. G., Anderson, M. C., Belward, A. S., Cohen, W. B., Dwyer, J., Erb, A., Gao, F., Gri, P., Helder, D., Hermosilla, T., Hipple, J. D., Hostert, P., Hughes, M. J., ... Zhu, Z. (2019). *Remote Sensing of Environment Current status of Landsat program , science , and applications*. 225(November 2018), 127–147. <https://doi.org/10.1016/j.rse.2019.02.015>
  58. Yang, Z., Wang, L., Sun, W., Xu, W., Tian, B., Zhou, Y., ... & Chen, C. (2022). A new adaptive remote sensing extraction algorithm for complex muddy coast waterline. *Remote Sensing*, 14(4), 861.
  59. Yasir, M., Hui, S., Binghu, H., & Rahman, S. U. (2020). Coastline extraction and land use change analysis using remote sensing (RS) and geographic information system (GIS) technology – A review of the literature. *Reviews on Environmental Health*, 35(4), 453–460. <https://doi.org/10.1515/reveh-2019-0103>
  60. Yu, J., Fu, Y., Li, Y., Han, G., Wang, Y., Zhou, D., Sun, W., Gao, Y., & Meixner, F. X. (2011). Effects of water discharge and sediment load on evolution of modern Yellow River Delta, China, over the period from 1976 to 2009. *Biogeosciences*, 8(9), 2427–2435. <https://doi.org/10.5194/bg-8-2427-2011>
  61. Zhang, X. K., Zhang, X., Lan, Q. Q., & Ali Baig, M. H. (2012). Automated detection of coastline using Landsat TM based on water index and edge detection methods. *Proceedings of the 2nd International Workshop on Earth Observation and Remote Sensing Applications, EORSA 2012, August 2012*, 153–156. <https://doi.org/10.1109/EORSA.2012.6261155>
  62. Zhou, X., Wang, J., Zheng, F., Wang, H., & Yang, H. (2023). An Overview of Coastline Extraction from Remote Sensing Data. *Remote Sensing*, 15(19). <https://doi.org/10.3390/rs15194865>